THE SOUTHERN SUPERCLUSTER

SHYAMAL MITRA
Department of Astronomy, University of Texas, Austin, Texas 78712
Received 20 April 1989; revised 1 June 1989

ABSTRACT

The Southern Supercluster is the closest supercluster to the Local Supercluster. The densest region of this supercluster lies between supergalactic longitudes 200° and 310° and supergalactic latitudes − 38° to − 45°, which correspond to right ascensions of 2 to 6 hr and declinations of + 5° to − 69°. From the contour maps made of galaxies from the *Second Reference Catalogue of Bright Galaxies* (RC2), two regions, A ($180° \leqslant L \leqslant 320°$, $-30° \geqslant B \geqslant -50°$) and B ($260° \leqslant L \leqslant 360°$, $0° \geqslant B \geqslant -30°$), were delineated for detailed study. Galaxies from five catalogs were compiled and the basic parameters, diameters and axis ratios, were reduced to the RC2 system. Magnitudes measured for 105 galaxies, most of them new, are presented. The magnitudes for other galaxies were obtained from the RC3 (in preparation). The radial velocities were culled from the literature. A self-consistent distance scale was established using tertiary distance indicators—the luminosity index Λ_c and the maximum rotation velocity $\log V_m$ obtained from H I linewidths. The distance moduli were obtained using parameters $\log D_0$ and B_T^0. The distance moduli derived from the central velocity dispersion of early-type galaxies, diameters of inner rings, and the method of "sosie" galaxies were obtained from other catalogs. A database was assembled containing several parameters like $\log D$, B_T^0, μ, V, etc. A statistical study of their distribution was made and a measure of their completeness estimated. It was shown for galaxies brighter than 14.0 mag that the probability that this areal distribution could have arisen by chance was less than 10^{-3}. Several maps were constructed to investigate the structure of the supercluster in three dimensions using the positional coordinates and a distance estimate from the radial velocity. The extent, size, and shape of the supercluster were determined. The supercluster lies within the velocity range 560–2240 km/s and has a velocity dispersion of 345 km/s. It is 41 Mpc along its longest dimension and is at a mean distance of 20 Mpc. Fifteen groups belonging to the supercluster were identified. The mass, luminosity, and mass-to-light ratio of the groups were computed. The mean mass-to-light ratio was $100h$ ($h = H/100$). The total luminosity of the supercluster was estimated to be $2.4 \times 10^{12} h^{-2} L_\odot$ after making corrections for incompleteness. The total mass of the supercluster was estimated to be $2.4 \times 10^{14} h^{-1} \mathcal{M}_\odot$. The Southern Supercluster is comparable to the Coma and Hercules superclusters in terms of mass and luminosity. Even though the Southern Supercluster is the nearest supercluster to the Local Supercluster, the two are not physically linked. However, there seems to be a tenuous connection between the Southern Supercluster and the Perseus Supercluster.

I. INTRODUCTION

The Southern Supercluster is a long chain of galaxies, the densest region of which passes through the constellations of Cetus, Fornax, Eridanus, Horologium, and Dorado. Even as early as 1847, John Herschel had pointed out the existence of this stream of galaxies. But it was only in 1953 that de Vaucouleurs recognized this band as a supercluster.

This supercluster at a mean distance of 20 Mpc is the nearest supercluster to the Local Supercluster. The Fornax Cluster and nearby groups in the region of the Southern Supercluster have been the subjects of study for several astronomers (Welch *et al.* 1975; Jones *et al.* 1980; Richter *et al.* 1985), but the Southern Supercluster as an entity has not been studied before.

The aim of this study was manifold. We wanted to determine whether the Southern Supercluster is in reality a cluster of clusters and not just a chance superposition of galaxies. Once this reality was established, we wanted to study its overall structure, determine the luminosity function, and estimate its total mass. We were also interested in possible connections of the Southern Supercluster with its neighbors.

II. PRELIMINARY STUDIES

For a preliminary analysis, galaxies from the *Second Reference Catalogue of Bright Galaxies* (de Vaucouleurs *et al.* 1976: RC2) were used. The data in the RC2 are homogeneous, but this catalog is not complete either to a limiting diameter or magnitude of interest. Consequently, the analysis has been affected by the lack of completeness.

The apparent distribution of galaxies was first studied in the supergalactic system restricted to the quadrant ($180° \leqslant L \leqslant 360°$, $0° \geqslant B \geqslant -90°$) in which the Southern Supercluster is located (Fig. 1). Using the plotting package AIPS, contour plots of the number counts of galaxies were produced. The canonical Southern Supercluster, as defined by de Vaucouleurs (1953, 1956), was in the region "$180° \leqslant L \leqslant 320°$, $-30° \geqslant B \geqslant -50°$" and was designated as Region A in our nomenclature. The contour plots also showed regions of high density connecting the Southern Supercluster to the supergalactic equator. We decided to investigate whether the galaxies in this region were an extension of the Southern Supercluster towards the Local Supercluster or the Perseus Supercluster. The boundaries of this region were "$260° \leqslant L \leqslant 360°$, $0° \geqslant B \geqslant -30°$" and was called Region B.

Is the areal distribution that de Vaucouleurs has called the Southern Supercluster due to a random fluctuation in the distribution of galaxies on the sky? A statistical analysis was performed to answer this question. The RC2 galaxies in the quadrant $180° \leqslant L \leqslant 360°$, $0° \geqslant B \geqslant -90°$ were binned according to magnitude (B_T). In each magnitude bin the observed number of galaxies was compared with the expected number of galaxies had the distribution been random. The probability that the observed number could arise in a Poisson distri-

 0004-6256/89/041175-13$00.90

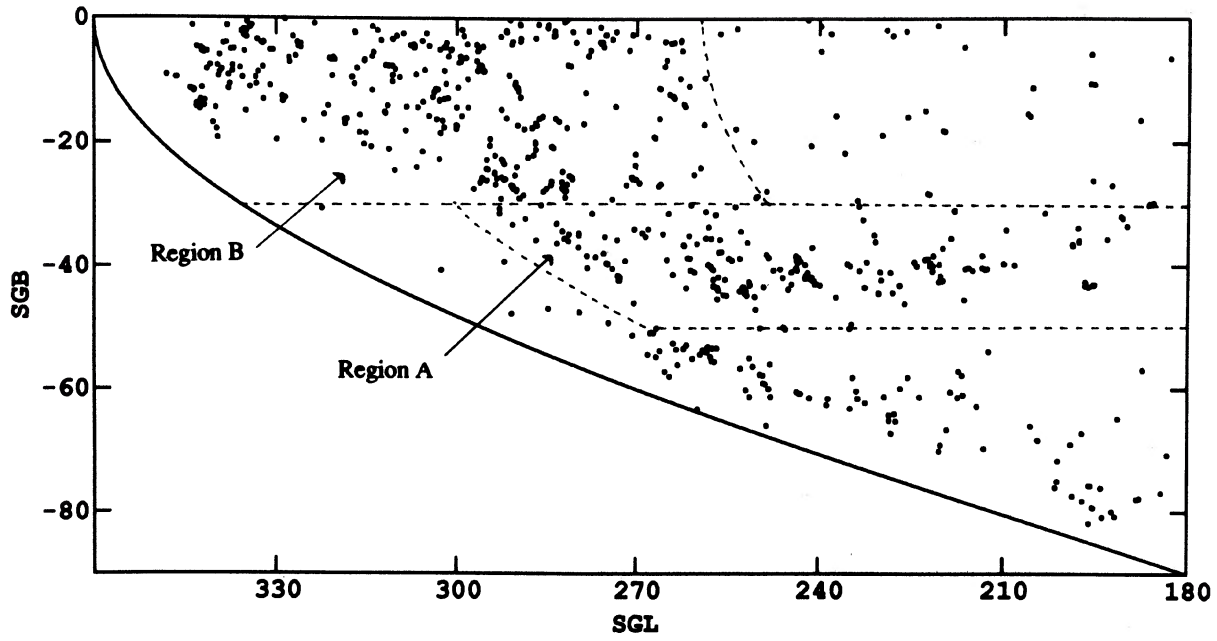

FIG. 1. The Southern Supercluster in supergalactic coordinates: Regions A and B defined.

bution was calculated for Region A, Region B, and the two regions combined.

The probability that a galaxy will fall randomly in Region A (for example) is $p = f_R = 0.21$. The probability that N of them will fall at random in Region A for a sample of size N_T is given by the Poisson function

$$P(N,\lambda) = \lambda^N e^{-\lambda}/N!,$$

where λ is the expectation of N, $\lambda = p N_T$. The probability that at least N galaxies will be in Region A is given by the cumulative function

$$F(N,\lambda) = \sum_N^{N_T} P(N,\lambda) = \sum_N^{N_T} P(N,pN_T).$$

Since N was large for many of the magnitude bins, Stirling's approximation was used for $N!$:

$$N! \approx \sqrt{2\pi N}\, e^{-N} N^N.$$

Hence,

$$P(N,\lambda) = \frac{1}{\sqrt{2\pi N}} \exp(N \ln \lambda - \lambda + N - N \ln N).$$

Table I gives the probabilities of obtaining N galaxies out of a sample of size N_T in the two regions and in various magnitude intervals. The relative frequency of the observed distribution is $f = N/N_T$, whereas the random frequency is f_R (without correction for extinction).

From Table I we can see that the probability of bright galaxies ($B_T \leqslant 13.0$) falling by chance in Region A is very small. On the contrary, the probability of faint galaxies ($B_T > 13.0$) falling at random in Region B is exceedingly small. This is consistent with the fact that the part of the supercluster in Region A is closer to us than the part in Region B. Thus the areal maps show the two regions to be statistically significant.

TABLE I. Poisson distribution probabilities for the Southern Supercluster.

	A	B	A+B	N_T
$B_T \leq 12.0$				
N	54	40	94	115
f	0.47	0.35	0.82	
f/f_R	2.24	1.24	1.70	
F	1.18×10^{-7}	0.10	1.27×10^{-6}	
$12.0 < B_T \leq 12.5$				
N	30	27	57	70
f	0.43	0.39	0.81	
f/f_R	2.04	1.38	1.70	
F	3.04×10^{-4}	6.53×10^{-2}	1.46×10^{-4}	
$12.5 < B_T \leq 13.0$				
N	26	30	56	75
f	0.35	0.40	0.75	
f/f_R	1.65	1.43	1.56	
F	1.10×10^{-2}	3.75×10^{-2}	1.21×10^{-3}	
$13.0 < B_T \leq 13.5$				
N	17	38	55	74
f	0.23	0.51	0.74	
f/f_R	1.09	1.83	1.55	
F	0.39	4.21×10^{-4}	1.46×10^{-3}	
$13.5 < B_T \leq 14.0$				
N	13	44	57	67
f	0.19	0.66	0.85	
f/f_R	0.92	2.35	1.77	
F	0.65	4.80×10^{-7}	4.83×10^{-5}	
f_R	0.21	0.28	0.48	

A comprehensive list of galaxies for the two regions was compiled from five catalogs—RC2, *Southern Galaxy Catalogue* (SGC), *Uppsala General Catalogue of Galaxies* (UGC), *Catalogue of Selected non-UGC Galaxies* (UGCS), and the *ESO / Uppsala Survey of the ESO(B) Atlas* (ESO). The source material for the catalogs was different and they also had different degrees of completeness. The data from the several catalogs were reduced to a homogeneous system following RC2. In spite of having five catalogs for reference, a large region of the sky between declinations $-2°$ and $-17°$ was undersampled because of a lack of a detailed survey in this area. The list contained galaxies having diameter ($\log D_{25}$), axis ratio ($\log R_{25}$), morphological type (T), luminosity class (L), total magnitude (B_T), and radial velocity (V).

The radial velocities were obtained primarily from the RC2 and the *Catalogue of Radial Velocities of Galaxies* by Palumbo *et al.* (1983). Dr. John Huchra kindly supplied some of the unpublished data from the CfA redshift catalog. The heliocentric radial velocities were reduced to the reference frame tied to the microwave background radiation. The velocity so calculated was called the corrected velocity V_c. In subsequent analysis, only the corrected velocity V_c was used.

III. OBSERVATIONS

Total magnitudes (B_T) were needed to derive the distance moduli of galaxies and the luminosity function for the supercluster. Some of the total magnitudes were obtained from the *Third Reference Catalogue of Bright Galaxies* (RC3, in preparation). Others were determined from multiple-aperture photometry performed at McDonald Observatory and at CTIO during the years 1983–1985.

The 0.91 and the 0.76 m telescopes were used at McDonald Observatory. On the 0.91 m telescope a 1P21 photomultiplier tube was used, whereas on the 0.76 m telescope the detector was a 56DVP photomultiplier tube. At CTIO the 0.91 m telescope with an RCA31034 tube was used for observations. The standard Johnson U, B, V filters were used for all the observations. A copper sulfate filter was used in conjunction with the U filter to eliminate the red leak. Most of the galaxies had magnitude measurements in three apertures. The total magnitude (B_T), total colors [$(B-V)_T$, $(U-B)_T$], and their respective mean errors were determined according to the precepts in RC2. Most of the observations were new, with some galaxies observed by other astronomers. From the sample of common galaxies, the external mean errors determined for the magnitude in the V filter and the colors ($B-V$) and ($U-B$) were 0.07, 0.05, and 0.06, respectively. Table II gives a list of the galaxy names, the logarithm of the size of the aperture, the observed V magnitude, the colors $B-V$ and $U-B$, the date, and the telescope used. The size of the aperture was measured in units of 0.1′ arc. The symbol "?" next to a reading indicates that its value is uncertain. An asterisk in the last column indicates there are comments in the section headed Notes.

IV. DISTANCE SCALE

The distance moduli for the galaxies in the Southern Supercluster were obtained from tertiary distance indicators. The two distance indicators that were primarily used were the luminosity index Λ_c (de Vaucouleurs 1979) and the maximum rotation velocity $\log V_m$ (Tully and Fisher 1977; Bottinelli *et al.* 1983) derived from H I linewidths. The distance moduli obtained from the B band Tully–Fisher relation were restricted to galaxies having inclinations $i \geqslant 35°$ and with morphological types in the range $2 \leqslant T \leqslant 8$. The distance indicators were used with the distance parameters $\log D_0$ and B_T^0 to derive the distance moduli. The slope adopted for the distance scale based on the luminosity index was 3.0, and for the distance scale based on $\log V_m$ the slope was 5.0. These were the values for the slope as used by previous investigators. However, the zero points for the two distance scales were adjusted to be the same. The equations used to derive the distance moduli were

$$\mu(\Lambda_c, D_0) = 38.71 - 5 \log D_0 - 3(\Lambda_c - 1),$$

$$\mu(\Lambda_c B_T^0) = 19.30 + B_T^0 - 3(\Lambda_c - 1),$$

$$\mu(V_m, D_0) = 38.71 - 5 \log D_0 + 5(\log V_m - 2.09),$$

$$\mu(V_m, B_T^0) = 19.30 + B_T^0 + 5(\log V_m - 2.09).$$

Tully (private communication) has pointed out that with a slope of 5 for the T–F relation there is certainly a Malmquist bias in the sample. To reduce the effects of Malmquist bias, only galaxies satisfying the criteria (i) $0.35 \leqslant \Lambda_c < 1.20$ or (ii) $\log V_m \geqslant 1.95$ were selected. Moreover, those galaxies having $\sigma(\Lambda_c) \geqslant 0.20$ or $\sigma(\log V_m) \geqslant 0.10$ were rejected.

There were other sources of distance moduli that were independent of Λ_c and $\log V_m$. These were from tertiary distance indicators—(i) central velocity dispersion (Faber and Jackson 1976; de Vaucouleurs and Olson 1982), (ii) diameter of inner rings (de Vaucouleurs and Buta 1980a,b), (iii) "sosie galaxies" (Paturel 1981). These distance moduli were not calculated but were culled from the literature. The zero points of the distance moduli culled from the literature were adjusted (by adding 0.24 mag) so that these distance moduli were consistent with the distance scale based on Λ_c and $\log V_m$. For galaxies having distance moduli from more than one distance indicator, a weighted mean was calculated with weights proportional to the inverse square of the mean errors.

V. COMPLETENESS OF THE DATABASE

All the measured parameters for the galaxies in the Southern Supercluster were reduced to a uniform system, and a comprehensive list was compiled. The final database consisted of the following items:

(1) Position of a galaxy in 1950.0 equatorial coordinates,
(2) The NGC, IC, or Anonymous designations (if there were any),
(3) A source code giving information regarding the catalog(s) in which a galaxy is listed,
(4) The diameter expressed as $\log D_{25}$ in the RC2 system,
(5) The axis ratio expressed as $\log R_{25}$ in the RC2 system,
(6) The mean morphological type T and its error $\sigma(T)$,
(7) The mean luminosity class L and its error $\sigma(L)$,
(8) The total magnitude B_T and its error $\sigma(B_T)$,
(9) The corrected radial velocity V_c and its mean error $\sigma(V_c)$,
(10) The corrected luminosity index Λ_c and its mean error $\sigma(\Lambda_c)$,
(11) The maximum rotation velocity expressed as $\log V_m$ and its mean error $\sigma(\log V_m)$,
(12) The distance moduli μ and its mean error $\sigma(\mu)$.

The statistics for the relevant parameters needed for the analysis are shown in Table III for Region A, Region B, and the two regions combined. Only if one makes the assumption that the galaxies are distributed uniformly in space can the

TABLE II. Observed magnitudes and colors of galaxies.

Name	log A	V	B-V	U-B	Date(UT)	Tel	Notes
N0101	0.75	14.22	0.66	0.01	841225	3	
	1.05	13.38	0.59	-0.08	841225	3	
	1.20	13.10	0.57	-0.01?	841225	3	*
N0172	0.75	14.92	0.64	0.21	841226	3	
	1.05	14.22	0.59	0.07	841226	3	
	1.20	13.88	0.62	0.00	841226	3	
N0268	0.74	13.91	0.63	-0.07	841001	1	
	1.05	13.22	0.52	-0.11	841001	1	
	1.34	13.07	0.56	-0.17	841001	1	
N0273	0.74	13.48	1.02	0.56	851208	1	
	1.05	13.14	0.97	0.53	851208	1	
	1.34	13.03	0.95	0.31?	851208	1	*
N0309	0.74	13.96	0.88	0.30	841001	1	
	1.05	12.91	0.78	0.09	841001	1	
	1.34	12.27	0.65	-0.01	841001	1	
N0352	0.74	13.43	1.12	0.41	851209	1	
	1.05	12.76	1.09	0.55	851209	1	
	1.34	12.19	1.49	0.39	851209	1	
N0418	0.75	13.91	0.81	0.13	841225	3	
	1.05	13.17	0.64	0.08	841225	3	
	1.20	12.86	0.62	-0.04	841225	3	
N0473	0.74	13.19	0.82	0.16	851208	1	
	1.05	12.82	0.83	0.21	851208	1	
	1.34	12.63	0.83	0.17	851208	1	
N0497	0.74	13.95	0.99	0.38	851209	1	
	1.05	13.29	0.90	0.32	851209	1	
	1.34	13.07	0.84	0.24	851209	1	
N0522	0.80	14.06	1.11	0.44	851014	2	
	1.10	13.45	1.07	0.58?	851014	2	
	1.41	13.05	1.01	0.29	851014	2	
N0532	0.80	13.96	1.04	0.61	851014	2	
	1.10	13.28	0.99	0.77	851014	2	
	1.41	12.89	1.12?	0.84	851014	2	
N0568	0.75	13.58	1.00	0.44	841225	3	
	1.05	13.16	1.01	0.51	841225	3	
	1.20	12.96	1.01	0.51	841225	3	
N0570	0.74	13.65	0.97	0.49	851213	1	
	1.05	13.18	0.98	0.44	851213	1	
	1.34	12.97	0.90	0.44	851213	1	
N0600	0.74	14.46	0.74	0.07	851213	1	
	1.05	13.49	0.64	-0.03	851213	1	
	1.34	12.74	0.61	-0.04	851213	1	
N0623	0.75	13.50	1.04	0.54	841226	3	
	1.05	13.07	1.08	0.54	841226	3	
	1.20	12.87	1.04	0.59?	841226	3	
N0658	1.05	13.10	0.69	-0.01	841020	1	
	1.34	12.70	0.65	-0.04	841020	1	*
N0661	0.74	12.90	1.00	0.53	841019	1	
	1.05	12.54	1.00	0.50	841019	1	
	1.34	12.25	0.99	0.46	841019	1	
N0668	0.74	13.73	0.74	0.12	841019	1	
	1.05	13.26	0.71	0.16	841019	1	
	1.34	13.11	0.69	0.10	841019	1	
N0669	0.74	13.45	1.13	0.60	841019	1	
	1.05	12.84	1.07	0.56	841019	1	
	1.34	12.47	1.08	0.52	841019	1	
N0670	0.74	13.18	0.88	0.22	841019	1	
	1.05	12.85	0.87	0.24	841019	1	
	1.34	12.76	0.86	0.25	841019	1	
N0673	0.74	13.85	0.75	0.05	851213	1	
	0.80	13.61	0.70	0.02	851013	2	
	1.05	12.97	0.65	-0.04	851213	1	
	1.10	12.88	0.63	-0.06	851013	2	
	1.34	12.64	0.64	-0.05	851213	1	
	1.41	12.67	0.63	-0.05	851013	2	
N0678	0.74	13.02	1.23	0.63	841019	1	
	1.05	12.64	1.17	0.62	841019	1	
	1.34	12.48	1.14	0.66	841019	1	
N0680	0.80	12.51	1.03	0.56	851013	2	
	1.10	12.17	1.03	0.47	851013	2	
	1.41	11.98	1.05	0.47	851013	2	
N0684	0.74	13.26	1.10	0.55	841020	1	
	1.05	12.83	1.06	0.54	841020	1	
	1.34	12.53	1.00	0.41	841020	1	
N0691	0.74	13.55	1.02	0.46	851218	1	
	1.05	12.78	0.98	0.38	851218	1	
	1.34	12.15	0.90	0.29	851218	1	*
N0693	0.74	13.27	0.83	0.12	851214	1	
	1.05	12.74	0.81	0.13	851214	1	
	1.34	12.51	0.81	0.14	851214	1	
N0701	0.74	13.35	0.75	0.04	841001	1	
	1.05	12.57	0.70	-0.02	841001	1	
	1.34	12.22	0.69	0.06	841001	1	
N0706	0.74	13.46	0.71	0.10	851215	1	
	1.05	12.76	0.69	0.07	851215	1	
	1.34	12.50	0.76	0.10	851215	1	*
N0748	0.74	13.56	0.97	0.41	851214	1	
	1.05	12.99	0.87	0.30	851214	1	
	1.34	12.72	0.81	0.21	851214	1	
N0755	0.74	13.65	0.60	-0.09	851218	1	
	1.05	12.96	0.58	-0.16	851218	1	
	1.34	12.68	0.52	-0.04	851218	1	
N0803	0.74	13.72	0.90	0.15	851219	1	
	1.05	13.06	0.76	0.05	851219	1	
	1.34	12.66	0.73	0.02	851219	1	*
N0828	0.74	13.45	0.94	0.36	851214	1	
	0.80	13.31	0.90	0.45	851013	2	
	1.05	12.88	0.94	0.42	851214	1	
	1.10	12.79	0.93	0.36	851013	2	
	1.34	12.51	0.89	0.37	851214	1	
	1.41	12.51	0.92	0.39	851013	2	
N0840	0.74	14.16	0.96	0.40	851215	1	
	1.05	13.67	0.94	0.25	851215	1	
	1.34	13.45	0.91	0.10?	851215	1	
N0841	0.80	13.08	0.95	0.34	851014	2	
	1.10	12.74	0.84?	0.36	851014	2	
	1.41	12.61	0.89	0.21?	851014	2	
N0881	0.74	13.68	0.90	0.35	851215	1	
	1.05	12.93	0.86	0.25	851215	1	
	1.34	12.55	0.82	0.26	851215	1	
N0897	0.75	13.02	1.01	0.59	841225	3	
	1.05	12.43	1.00	0.49	841225	3	
	1.20	12.18	0.98	0.51	841225	3	
N0910	0.74	13.20	1.06	0.51	841020	1	
	1.05	12.78	1.04	0.53	841020	1	
	1.34	12.41	1.02	0.51	841020	1	
N0918	0.74	14.22	1.04	0.29	851219	1	
	1.05	13.26	0.96	0.38?	851219	1	
	1.34	12.51	0.92	0.19	851219	1	
N0926	0.74	14.11	0.84	0.33	851216	1	
	1.05	13.47	0.80	0.24	851216	1	
	1.34	13.26	0.80	0.18	851216	1	
N0941	0.74	13.99	0.54	-0.16	841019	1	
	1.05	13.19	0.53	-0.17	841001	1	
	1.05	13.20	0.53	-0.15	841019	1	
	1.34	12.74	0.52	-0.13	841001	1	
N0945	0.75	13.60	0.88	0.29	841226	3	
	1.05	12.82	0.81	0.18	841226	3	
	1.20	12.49	0.79	0.17	841226	3	
N0947	0.75	13.90	0.77	0.15	841226	3	
	1.05	13.16	0.65	0.07	841226	3	
	1.20	12.91	0.62	-0.05	841226	3	
N0959	0.74	13.91	0.61	-0.10	851216	1	
	1.05	12.92	0.60	-0.13	851216	1	
	1.34	12.55	0.60	-0.04	851216	1	
N0976	0.74	13.03	0.90	0.23	841001	1	
	1.05	12.66	0.85	0.15	841001	1	
	1.34	12.48	0.87	0.21	841001	1	
N1016	0.74	12.90	1.07	0.62	851218	1	
	1.05	12.37	1.06	0.60	851218	1	
	1.34	11.99	1.04	0.61	851218	1	*
N1024	0.74	13.07	1.14	0.63	851214	1	
	1.05	12.64	1.07	0.37	851214	1	
	1.34	12.29	1.03	0.49?	851214	1	*
N1091	0.74	14.60	0.92	0.36	851216	1	
	1.05	14.19	1.04	0.33	851216	1	
	1.34	14.17	0.86	0.37	851216	1	
N1092	0.74	13.92	1.01	0.37	851218	1	
	1.05	13.57	1.05	0.39	851218	1	
	1.34	13.49	1.05	0.49?	851218	1	
N1098	0.75	13.40	1.01	0.47	841227	3	
	1.05	12.99	1.01	0.38	841227	3	
	1.20	12.84	0.98	0.37	841227	3	
N1099	0.74	13.97	0.86	0.29	851215	1	
	1.05	13.43	0.87	0.26	851215	1	
	1.34	13.16	0.88	0.27	851215	1	
N1032	0.74	12.61	1.04	0.58	851213	1	
	1.05	12.13	1.02	0.54	851213	1	
	1.34	11.83	1.00	0.51	851213	1	
N1100	0.74	13.85	0.97	0.40	851215	1	
	1.05	13.36	0.93	0.31	851215	1	
	1.34	13.10	0.93	0.44?	851215	1	

TABLE II. (continued)

Name	log A	V	B-V	U-B	Date(UT)	Tel	Notes
N1125	0.74	13.43	0.87	0.21?	851219	1	*
	1.05	13.02	0.84	0.33	851219	1	*
	1.34	12.74	0.84	0.29	851219	1	*
N1145	0.74	13.99	1.11	0.26	851208	1	
	1.05	13.07	1.23	0.29?	851208	1	
	1.34	12.34	1.49	0.12	851208	1	
N1163	0.75	14.47	0.95	0.28	841226	3	
	1.05	13.96	0.92	0.17	841226	3	
	1.20	13.84	0.96	0.47?	841226	3	
N1194	0.74	13.80	1.07	0.55	851209	1	
	1.05	13.35	1.04	0.48	851209	1	
	1.34	13.07	0.97	0.50	851209	1	*
N1210	0.75	13.73	0.89	0.48	841227	3	
	1.05	13.30	0.87	0.34	841227	3	
	1.20	13.10	0.84	0.24	841227	3	
N1211	0.74	13.14	1.02	0.50	851218	1	
	1.05	12.75	0.95	0.44	851218	1	
	1.34	12.48	0.94	0.48	851218	1	
N1219	0.74	13.94	0.91	0.22	851215	1	
	1.05	13.24	0.81	0.23	851215	1	
	1.34	13.04	0.86	0.32	851215	1	
N1222	0.74	12.98	0.57	-0.19	831030	1	
	1.05	12.65	0.59	-0.14	831030	1	
	1.34	12.53	0.61	-0.05	831030	1	
N1241	0.74	13.24	1.09	0.34	831101	1	
	1.05	12.54	0.93	0.16	831101	1	
N1242	0.74	14.37	0.67	0.03	851215	1	
	1.05	14.02	0.66	0.04	851215	1	
	1.34	13.82	0.62	-0.12?	851215	1	
N1247	0.74	13.62	1.04	0.43	851209	1	*
	0.80	13.46	0.99	0.48	851013	2	
	1.05	13.04	1.01	0.41	851209	1	
	1.10	13.00	0.96	0.46	851013	2	
	1.34	12.62	1.03	0.31	851209	1	
	1.41	12.62	1.02	0.33	851013	2	
N1248	0.74	13.03	0.91	0.37	831031	1	
	1.05	12.70	0.87	0.34	831031	1	
	1.34	12.60	0.88	0.31	831031	1	
N1249	0.75	13.59	0.53	-0.07	841225	3	
	1.05	12.71	0.51	-0.12	841225	3	
	1.20	12.33	0.48	-0.13	841225	3	
N1250	0.74	13.62	1.16	0.64	851216	1	
	1.05	13.31	1.17	0.52	851216	1	
	1.34	12.90	1.11	0.28	851216	1	*
N1272	0.74	13.42	1.19	0.69	841020	1	
	1.05	12.84	1.14	0.59	841020	1	
	1.34	12.34	1.13	0.69	841020	1	
N1280	0.74	13.79	0.75	0.05	851219	1	
	1.05	13.45	0.70	0.02	851219	1	
	1.34	13.43	0.70	-0.04	851219	1	
N1289	0.74	13.34	1.02	0.44	851216	1	
	1.05	13.00	0.97	0.50	851216	1	
	1.34	12.70	0.96	0.56	851216	1	
N1298	0.74	14.48	0.98	0.60	831030	1	
	1.05	14.25	0.86?	0.35	831030	1	
	1.34	14.05	0.98	0.19	831030	1	
N1301	0.74	14.43	0.83	0.21	851208	1	
	1.05	13.63	0.80	0.15	851208	1	
	1.34	13.43	0.74	0.24?	851208	1	
N1305	0.74	13.51	1.10	0.56	831030	1	
	1.05	13.06	1.07	0.44	831030	1	
	1.34	12.46?	0.99	0.32	831030	1	*
N1310	0.75	13.73	0.65	-0.02	841226	3	
	0.75	13.75	0.63	-0.01	841227	3	
	1.05	12.97	0.59	-0.04	841226	3	
	1.05	12.92	0.57	-0.08	841227	3	
	1.20	12.63	0.57	-0.06	841227	3	
N1311	0.75	14.22	0.44	-0.29	841224	3	
	1.05	13.39	0.45	-0.25	841224	3	
	1.20	13.09	0.48	-0.26	841224	3	
N1320	0.74	13.16	0.89	0.25	831031	1	
	1.05	12.80	0.87	0.31	831031	1	
	1.34	12.52	0.89	0.26	831030	1	
N1329	0.74	13.50	0.90	0.41	851209	1	
	1.05	12.94	0.88	0.30	851209	1	
	1.34	12.72	0.86	0.30	851209	1	
N1336	0.75	13.52	0.86	0.33	841224	3	
	1.05	12.95	0.87	0.27	841224	3	
	1.20	12.74	0.86	0.30	841224	3	
N1349	0.74	14.13	1.18	0.66	851209	1	
	1.05	13.62	1.16	0.57	851209	1	
	1.34	13.30	1.14	0.48	851209	1	*
N1352	0.74	14.01	0.96	0.56	851213	1	
	1.05	13.70	0.97	0.44?	851213	1	
	1.34	13.48	0.93	0.56	851213	1	*
N1383	0.75	13.07	0.99	0.46	841227	1	
	1.05	12.70	1.00	0.37	841227	1	*
	1.20	12.62	0.98	0.40	841227	1	*
N1391	0.74	13.84	1.05	0.52	851214	1	
	1.05	13.52	1.01	0.45	851214	1	
	1.34	13.38	1.03	0.39	851214	1	
N1393	0.74	12.94	0.97	0.59	831030	1	
	0.74	12.99	0.97	0.50	831031	1	
	1.05	12.37	0.98	0.45	831030	1	
	1.05	12.46	0.96	0.51	831031	1	
	1.34	12.17	0.94	0.47	831030	1	
N1394	0.74	13.37	1.03	0.57	851215	1	
	1.05	13.08	1.04	0.49	851215	1	
	1.34	12.94	0.98	0.40	851215	1	
N1401	0.75	12.89	0.91	0.41	841226	3	
	0.75	12.92	0.91	0.44	841227	3	
	1.05	12.54	0.88	0.41	841226	3	
	1.05	12.57	0.85	0.38	841227	3	
	1.20	12.43	0.86	0.42	841226	3	*
	1.20	12.43	0.86	0.35	841227	3	*
N1402	0.74	13.78	0.82	0.28	851216	1	
	1.05	13.59	0.81	0.13	851216	1	
	1.34	13.70	0.71	0.29	851216	1	
N1424	0.74	14.36	0.62	-0.05	851214	1	
	1.05	13.88	0.54	-0.09	831031	1	
	1.05	13.90	0.59	0.11	851214	1	
	1.34	13.85	0.46	-0.15	831031	1	
	1.34	13.80	0.61	-0.06	851214	1	
N1438	0.75	13.56	0.89	0.36	841227	3	
	1.05	12.79	0.86	0.29	841227	3	
	1.20	12.61	0.82	0.28	841227	3	
N1440	0.75	12.51	1.06	0.64	841224	3	
	1.05	12.06	1.04	0.62	841224	3	
	1.20	11.85	1.05	0.64	841224	3	
N1452	0.75	12.73	1.02	0.61	841227	3	
	1.05	12.31	1.00	0.61	841227	3	
	1.20	12.12	1.01	0.64	841227	3	
N1482	0.74	13.29	1.04	0.16	831101	1	
	1.05	12.72	0.99	0.14	831101	1	
	1.34	12.34	0.96	0.03?	831101	1	
N1484	0.75	14.36	0.58	0.07	841225	3	
	1.05	13.72	0.60	0.01	841225	3	
	1.20	13.47	0.54	0.11?	841225	3	
N1489	0.74	14.52	0.89	0.17	851214	1	
	1.05	14.00	0.86	0.06	851214	1	
	1.34	13.86	0.80	0.03	851214	1	
N1495	0.75	13.86	0.63	-0.01	841226	3	
	1.05	13.22	0.64	-0.02	841226	3	
	1.20	12.96	0.67	-0.11	841226	3	
N1519	0.74	14.18	0.59	0.01	851209	1	
	1.05	13.41	0.63	-0.07	851209	1	
	1.34	13.06	0.63	0.02	851209	1	
N1522	0.75	14.01	0.35	-0.40	841227	3	
	1.05	13.60	0.51	-0.30	841227	3	
	1.20	13.53	0.52	-0.30	841227	3	
N1541	0.74	13.97	1.11	0.47?	851209	1	
	1.05	13.66	1.06	0.73	851209	1	
	1.34	13.58	1.03	0.80	851209	1	*
N1556	0.75	13.66	0.42	-0.15	841227	3	
	1.05	13.18	0.42	-0.25	841227	3	
	1.20	13.14	0.42	-0.27	841227	3	
N1572	0.75	13.47	0.93	0.28	841224	3	
	1.05	12.90	0.89	0.25	841224	3	
	1.20	12.73	0.86	0.26	841224	3	
N1703	0.75	13.32	0.77	0.06	841225	3	
	1.05	12.37	0.66	-0.03	841225	3	
	1.20	11.94	0.62	-0.04	841225	3	
N1809	0.75	14.08	0.77	0.07	841224	3	
	1.05	13.20	0.79	0.17	841224	3	
	1.20	12.76	0.84	0.16	841224	3	
N1824	0.75	14.59	0.46	-0.18	841226	3	
	1.05	13.54	0.46	-0.10	841226	3	
	1.20	13.13	0.45	-0.13	841226	3	
N1892	0.75	13.48	0.62	-0.05	841225	3	
	1.05	12.80	0.61	-0.13	841225	3	
	1.20	12.49	0.60	-0.08	841225	3	
I0167	0.74	14.70	0.61	-0.16	841020	1	
	1.34	13.59	0.56	-0.26	841020	1	

TABLE II. (continued)

Name	log A	V	B-V	U-B	Date(UT)	Tel	Notes	Name	log A	V	B-V	U-B	Date(UT)	Tel	Notes
I0267	0.74	14.29	0.99	0.24	851218	1		I0346	0.74	14.01	0.90	0.49	851216	1	
	1.05	13.51	0.91	0.13	851218	1			0.80	13.75	0.92	0.57	851013	2	
	1.34	13.14	0.86	0.03	851218	1			1.05	13.31	0.96	0.45	851216	1	
I0302	0.74	14.31	1.03	0.49?	831031	1			1.10	13.13	0.99	0.53	851013	2	
	1.05	13.37	0.94	0.18	831031	1			1.34	13.05	0.94	0.97?	851216	1	
	1.34	12.92	0.85	0.15	831031	1			1.41	12.86	0.92	0.68	851013	2	
I0343	0.74	14.22	1.01	0.57	851218	1		I2085	0.75	14.17	0.87	0.24	841227	3	
	1.05	13.51	0.97	0.39	851218	1			1.05	13.74	0.82	0.45?s	841227	3	
	1.34	13.26	0.92	0.16	851218	1	*		1.20	13.52	0.82	0.23	841226	3	

Code for the telescopes - McDonald 0.91m : 1; McDonald 0.76m : 2; CTIO 0.91m : 3.

Notes to TABLE II

N0101	Corrected for star (V= 15.03, B-V = 0.72, U-B = 0.24)
N0273	Corrected for star (V = 14.70, B-V =0.73, U-B = 0.25)
N0658	Corrected for star (V = 16.60, B-V = 0.69, U-B = 0.42)
N0691	Corrected for star 1 (V = 16.15, B-V = 0.98, U-B = -0.06)
	Corrected for star 2 (V = 15.55, B-V = 1.05, U-B = 0.78)
	Not corrected for star 3 which was too faint to center
N0706	Corrected for star (V = 12.82, B-V = 0.88, U-B = 0.56)
N0803	Corrected for star 1 (V = 11.42, B-V = 0.68, U-B = 0.18)
	Not corrected for star 2 which was too faint to center
N1016	Corrected for star (V = 15.99, B-V = 0.72, U-B = -0.05)
N1024	Corrected for star (V = 12.27, B-V = 0.68, U-B = 0.08)
N1125	Corrected for star very close to the galaxy in all 3 apertures
	(V = 14.97, B-V = 0.58, U-B = 0.30)
N1194	Corrected for star 1 (V = 15.33, B-V = 0.78, U-B = 0.09)
	Corrected for star 2 (V = 16.03, B-V = 0.73, U-B = 0.19)
	Not corrected for other fainter stars in the field
N1247	Not corrected for a star close to the nucleus of the galaxy
N1250	Corrected for star (V = 15.03, B-V = 0.56, U-B = 0.05)
	Not corrected for other fainter stars in the field
N1305	Galaxy off-centered to avoid 2 stars
N1349	Corrected for star (V = 16.14, B-V = 0.71, U-B = 0.17)
N1352	Corrected for star 1 (V = 15.82, B-V = 0.72, U-B = -0.02)
	Corrected for star 2 (V = 16.62, B-V = 0.76, U-B = 0.14)
N1383	Corrected for star (V = 17.09, B-V = -0.10, U-B = 0.69)
N1401	Corrected for star (V = 13.81, B-V = 0.64, U-B = 0.07)
N1541	Not corrected some faint stars in the field
I0343	Corrected for star 1 (V = 15.87, B-V = 1.30, U-B = 0.69)
	Not corrected for star 2 which was too faint to center

completeness level be determined. Since nearly all the galaxies had a diameter measurement, the completeness was calculated in terms of log D. The logarithm of the cumulative frequency (N_D) of the number of galaxies bigger than a limiting diameter plotted against ($-5 \log D$) has a slope of 0.6. This fact was utilized in obtaining the "cosmic" value of the cumulative frequency N_c for a uniform distribution. The fraction of galaxies having the relevant parameters log D, B_T, V_c, and μ with respect to the cosmic value N_c was estimated as a function of log D. This fraction of galaxies was a measure of the incompleteness factor. The value of log D when the fraction is 0.5 gives the completeness at the 50% level. A linear relation between 5 log D and B_T was determined to convert the limiting diameters to magnitudes. The transformation equation was

$$B_T - 13.00 = -1.02[5(\log D - 1.39)]. \pm 0.03$$

Table IV gives both the limiting diameters and magnitudes at the 50% completeness level for the two regions separately and combined. This method cannot distinguish between the incompleteness that arises due to sampling and nonuniform distribution of galaxies. In carrying out the analyses, we made the assumption of a homogeneous universe (which we know is not true on the scale of superclusters) and we did not separate the galaxies belonging to the supercluster from those that do not. The numbers calculated for the completeness levels refer to the entire database and not to the supercluster proper.

The relevant parameters (the ones that were used for further analyses) were log D, B_T, V_c, and μ. The most complete parameter was log D and the least complete parameter was the distance modulus μ. Most of the catalogs attempted to be complete to log $D = 1.00$, or 1′ of arc in diameter. It was not surprising that the 50% completeness level for log D was close to that value. The limiting log D value was 1.01, which corresponded to an apparent magnitude of ~15. The next most complete parameter was the radial velocity. It was complete at the 50% level at log $D = 1.22$, or 1.7′ of arc in diameter or 13.9 mag. Most of the bright galaxies had a mea-

TABLE III. Statistics of the sample.

Parameter	Reg A	Reg B	Reg A + B
Log D	2223	2895	5118
B_T	208	231	439
Vel	552	1114	1666
μ	260	354	614

TABLE IV. Log D and B_T at the 50% completeness level.

Parameter	Reg A		Reg B		Reg A + B	
	Log D	B_T	Log D	B_T	Log D	B_T
Log D	0.94	15.33	0.94	15.32	0.95	15.25
B_T	1.37	12.96	1.39	13.19	1.40	12.95
Vel	1.26	13.57	1.12	14.47	1.18	14.07
μ	1.41	12.75	1.43	13.01	1.44	12.74

sure of their total magnitude but not so with the faint ones. The 50% completeness level for B_T was 12.9 mag, which corresponds to $\log D = 1.41$, or 2.6′ of arc in diameter. A relatively small number of galaxies had a determination of distance modulus. The completeness at the 50% level was at $\log D = 1.49$, or 3.1′ of arc in diameter or 12.5 mag.

VI. STRUCTURE OF THE SOUTHERN SUPERCLUSTER

What does the Southern Supercluster look like? To describe the structure of a supercluster, one needs to study the distribution of galaxies with respect to coordinates and redshift. All sky plots were generated in overlapping velocity bins of 500 km/s which show the growth and dissolution of the supercluster. The structure manifests itself at 500 km/s, becomes quite prominent at 1500 km/s, and starts fading away at 2000 km/s.

The traditional way to study the structure of a supercluster is to make polar plots. Such plots were generated in wedges parallel and perpendicular to the supergalactic equator. Two representative plots for Region A are shown (Figs. 2 and 3). The supercluster is well defined in velocity space. There is a void beyond 2500 km/s, and it is only after 4000 km/s that aggregations of galaxies are seen. Three major clusters can be distinguished: Dorado, Fornax, and Eridanus. A part of the scatter is due to the velocity dispersion in the cluster ("the finger of God" effect), but a part of the spread must be due to the actual structure since the dispersion in velocity is not along radial lines only. Two representative plots are shown for Region B (Figs. 4 and 5). The supercluster can be distinguished even though this section of it lacks prominent clusters like the Fornax Cluster. The Perseus Supercluster can be seen in the background.

From the polar graphs, the range of the Southern Supercluster in velocity space was determined. The supercluster proper lies within the limits $560 \leqslant V_c$ km/s$\leqslant 2240$. To show quantitatively that the galaxies that form the Southern Supercluster are not due to random fluctuation in velocity space, the following statistical test was performed (see Rood 1975):

The Abell luminosity function $f(M)$ gives the fraction of galaxies per unit volume of space in a unit magnitude interval about absolute magnitude M:

$$f(M) = k_1 \,\mathrm{dex}(s_1 M), \qquad M_{\min} \leqslant M \leqslant M^*,$$

$$f(M) = k_1 \,\mathrm{dex}[s_1 M^* + s_2 (M - M^*)], \qquad M^* \leqslant M \leqslant M_{\max},$$

where k_1 is a normalization constant, $s_1 = 0.80$, $s_2 = 0.28$, and $M^* = -18.4$ (B band photoelectric magnitude on a distance scale of $H_0 = 100$ km/s/Mpc). In our sample $M_{\min} = -21.69$ and $M_{\max} = -12.56$. The limiting apparent magnitude m' of the sample was 14.0 mag. In order to facilitate calculations, $M_{\max}$ was set to ∞.

As we go further out in space we encounter more and more galaxies fainter than m'. Only galaxies brighter than absolute magnitude M' will appear brighter than m' for a given distance (or velocity) and hence be included in the sample.

$$M' = m' + 5 - 5 \log V/H.$$

For a limiting apparent magnitude of 14.0 and a minimum absolute magnitude of -21.69, the furthest distance one can observe corresponds to a velocity of 13 740 km/s. The radial velocity corresponding to absolute magnitude M^* is 3020 km/s, and for the maximum absolute magnitude $M_{\max} = -12.56$ the velocity is 205 km/s. Galaxies having velocities more than 3020 km/s will populate only the bright end of the luminosity function, whereas galaxies having veloc-

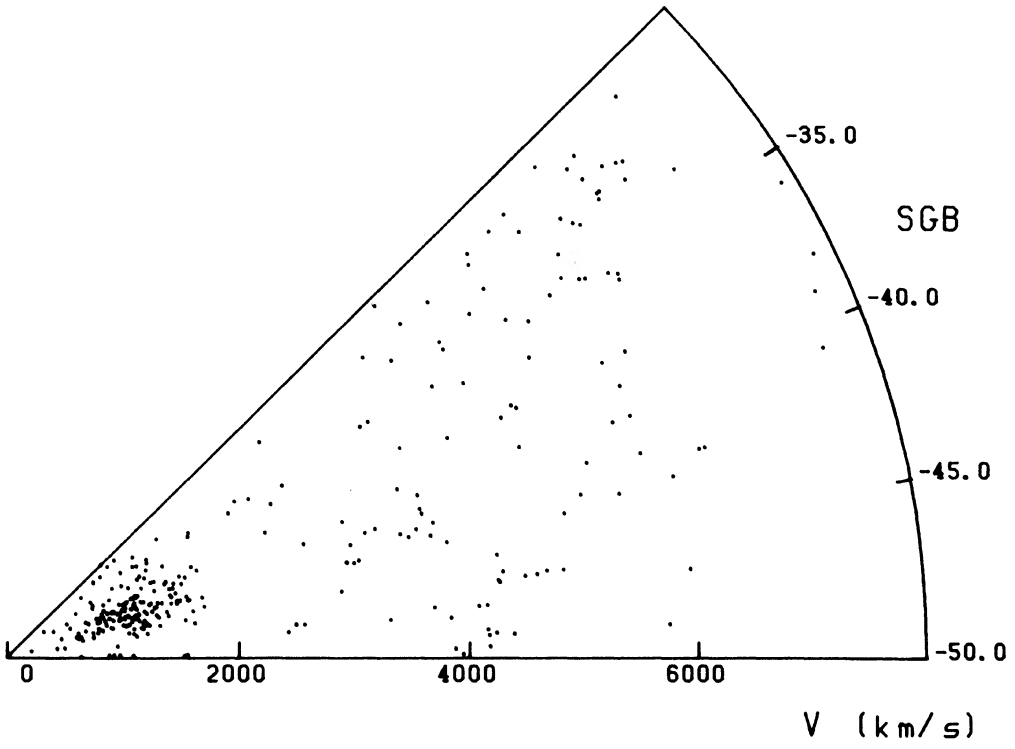

FIG. 2. Cone diagram perpendicular to the supergalactic equator for galaxies in Region A.

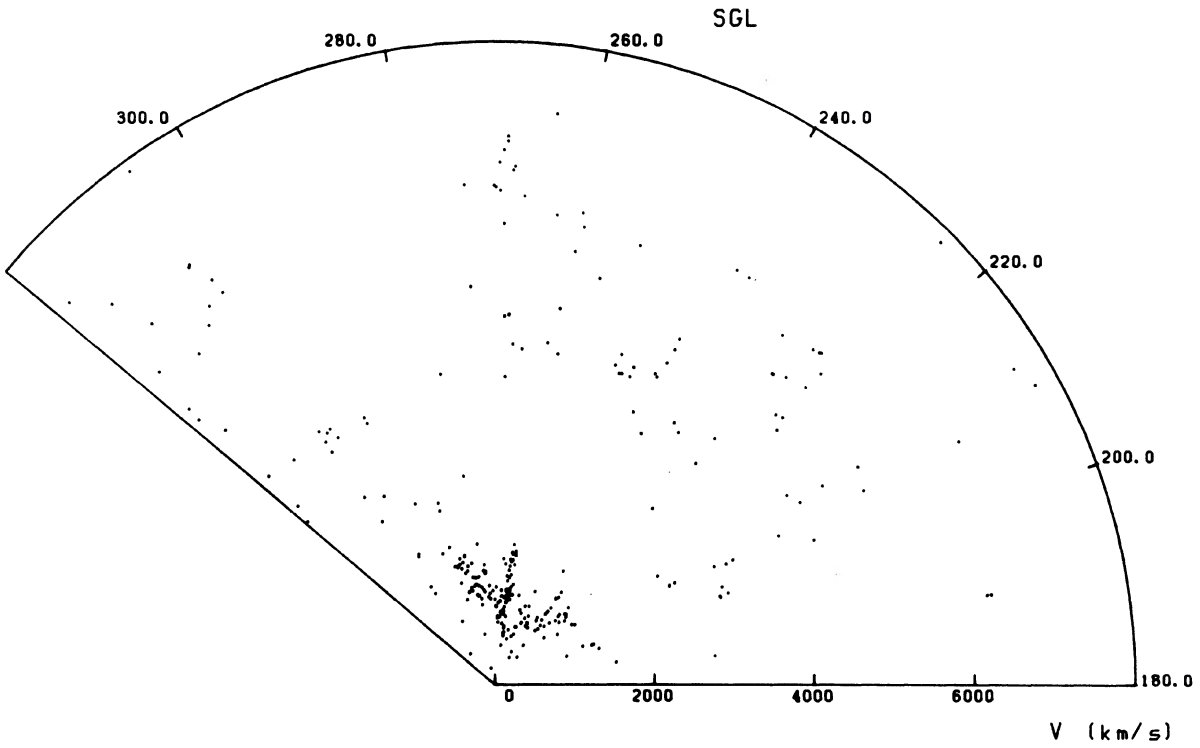

FIG. 3. Cone diagram parallel to the supergalactic equator for galaxies in Region A.

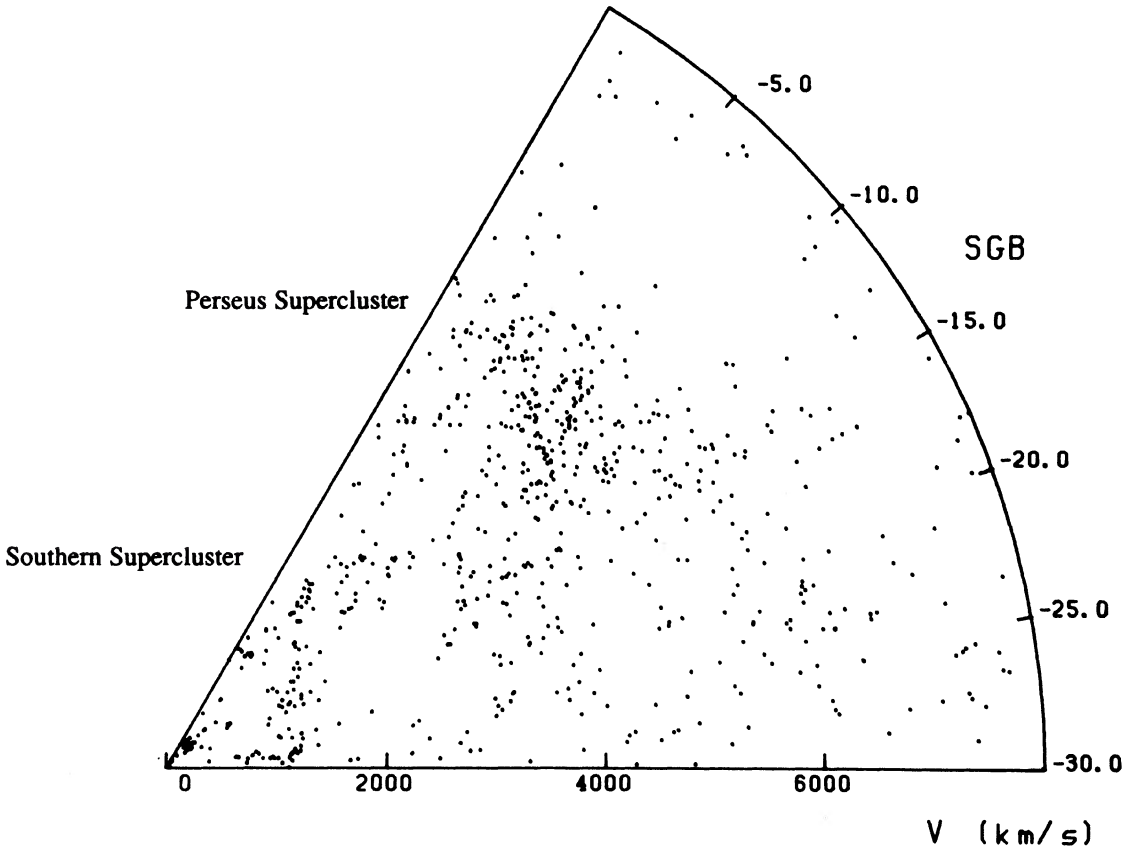

FIG. 4. Cone diagram perpendicular to the supergalactic equator for galaxies in Region B. Note the band of galaxies connecting the Southern and Perseus superclusters.

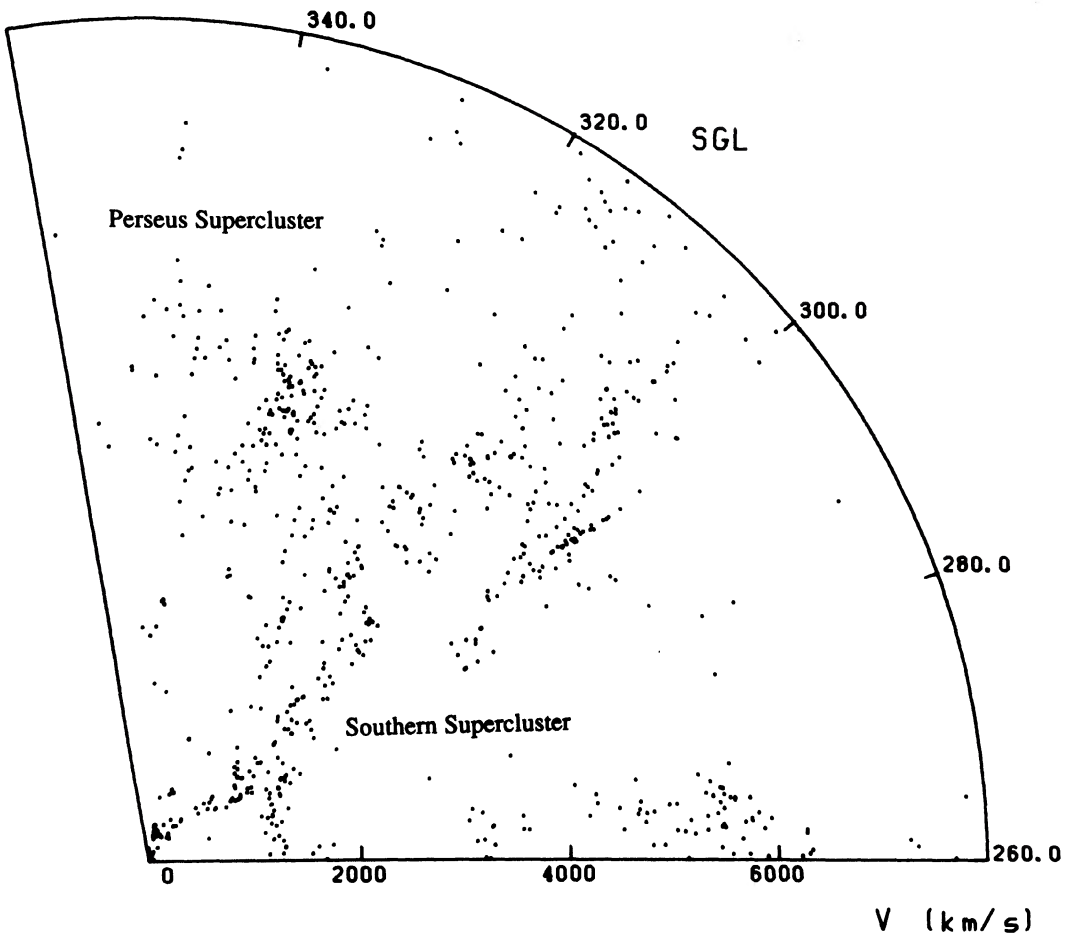

FIG. 5. Cone diagram parallel to the supergalactic equator for galaxies in Region B. Note that the band of galaxies connecting the Southern and Perseus superclusters is still evident.

ities less than 3020 km/s will populate both the bright and faint ends.

If galaxies were uniformly distributed in space, then the number of galaxies brighter than m' in a velocity interval dV about V is given by

$$N_f(V)dV = (4\pi V^2 dV)k \int_{M_{\min}}^{M'} f(M)dM,$$

where k is a normalization constant. The integral becomes smaller as V increases and is zero at $V = 13\,740$ km/s. The total number of galaxies in this velocity space is given by

$$\int_0^V N_f(V)dV = K\,[3.98\times10^{-9}V^{1.6} - 1.86\times10^{-14}V^3],$$

$$V < 3020 \text{ km/s}$$

$$\int_{3020}^V N_f(V)dV$$

$$= K\left[8.25\times10^{-4} - \frac{2.49}{V} - 2.33\times10^{-17}V^3\right],$$

$$V > 3020 \text{ km/s},$$

where K is the normalization constant. The total number of galaxies in the sample brighter than 14.0 mag was 308. The value of K was adjusted to give the same total number of galaxies for the homogeneous sample. Table V gives the observed and expected frequency distribution of galaxies. The statistic χ^2 was estimated

$$\chi^2 = \sum_i \frac{(o_i - e_i)^2}{e_i},$$

where o_i is the observed frequency and e_i is the frequency in the ith bin. The galaxies were rebinned such that in no bin was the expected number of galaxies less than 5.0. The hypothesis that the observed distribution occurred by chance has a probability of less than 10^{-3}.

The number of galaxies with $\log D \geqslant 1.00$ or $D \geqslant 1'$ of arc was obtained. From the B_T vs $\log D$ relation, the apparent magnitude corresponding to $\log D = 1.00$ was estimated to be $B_T = 15.0$ mag. The number of galaxies with redshifts that are brighter than 15th magnitude or bigger than 1' of arc in diameter was 378. From our study of the completeness of the various parameters, the incompleteness factor was determined. Dividing by the incompleteness factor, the expected number of galaxies within the supercluster becomes ~ 1500.

The supercluster has two segments. One segment which is in Region A lies parallel to the supergalactic plane. The ridge line is around latitude $-41°$. This segment is 83° in length.

TABLE V. Observed and expected distribution in velocity space.

Vel km/s	Obs	Exp	Vel km/s	Obs	Exp
0 - 250	6	5.7	7000 - 7250	0	2.3
250 - 500	11	10.7	7250 - 7500	1	2.1
500 - 750	13	14.0	7500 - 7750	1	1.9
750 - 1000	30	16.4	7750 - 8000	0	1.8
1000 - 1250	63	18.0	8000 - 8250	1	1.7
1250 - 1500	44	19.0	8250 - 8500	2	1.5
1500 - 1750	19	19.5	8500 - 8750	1	1.4
1750 - 2000	9	19.5	8750 - 9000	0	1.3
2000 - 2250	8	19.0	9000 - 9250	0	1.2
2250 - 2500	10	18.0	9250 - 9500	0	1.1
2500 - 2750	5	16.6	9500 - 9750	0	1.0
2750 - 3000	3	14.8	9750 - 10000	0	0.9
3000 - 3250	8	12.7	10000 - 10250	1	0.9
3250 - 3500	4	10.9	10250 - 10500	0	0.8
3500 - 3750	9	9.4	10500 - 10750	0	0.7
3750 - 4000	5	8.2	10750 - 11000	0	0.6
4000 - 4250	5	7.2	11000 - 11250	1	0.6
4250 - 4500	2	6.4	11250 - 11500	0	0.5
4500 - 4750	9	5.7	11500 - 11750	0	0.5
4750 - 5000	9	5.1	11750 - 12000	0	0.4
5000 - 5250	11	4.6	12000 - 12250	0	0.3
5250 - 5500	6	4.2	12250 - 12500	0	0.3
5500 - 5750	4	3.8	12500 - 12750	0	0.2
5750 - 6000	2	3.5	12750 - 13000	0	0.2
6000 - 6250	3	3.2	13000 - 13250	0	0.1
6250 - 6500	0	2.9	13250 - 13500	0	0.1
6500 - 6750	1	2.7	13500 - 13750	0	0.0
6750 - 7000	1	2.5			

The other segment in Region B is almost perpendicular to the supergalactic equator. The densest portion lies between the limits $270 \leqslant L \leqslant 320°$. The length of this section is 40°. Hence the total angular length of the supercluster is $\sim 123°$. The angular widths were estimated from number counts of galaxies in the velocity range of the supercluster proper. These counts were made in overlapping bins of 10° in supergalactic longitude while scanning perpendicular to the supergalactic equator, and 2° in supergalactic latitude while scanning parallel to the equator. Gaussian fits were made for the smoothed number-count profiles. The angular width of the supercluster in Region A was 9°, whereas it was 4 times wider (angular width of 36°) in Region B.

To transform the angular length and width to the corresponding linear length and width, one needs the mean distance of the subsections of the supercluster. The segment of the supercluster in Region A is slightly closer (19 Mpc) to us than the segment at 22 Mpc in Region B. The mean velocity of 1161 km/s in Region A is lower than the corresponding velocity of 1403 km/s in Region B. However, the mean Hubble ratios in the two segments are about the same ($H = 64$ km/s/Mpc).

Knowing the mean distance and the angular sizes, the linear sizes could be estimated. The total length of the supercluster is 41 Mpc. The mean width of the supercluster in Region A is 3 Mpc, whereas in Region B it is 13 Mpc. The thickness (depth) was estimated in two ways: (1) Using the dispersion in distance modulus, the thickness was taken to be $\pm 2\sigma$ from the mean distance; (ii) Using the velocity dispersion, the range in velocity was taken to be $\pm 2\sigma$ from the mean velocity. Then a distance range was calculated from the velocity range using the local value of the Hubble ratio. This distance range was taken to be the thickness. Note that the dispersion in distance modulus was due to the combined effect of the depth of the supercluster and the intrinsic mean error in the distance modulus. The same was true for the velocity dispersion. The intrinsic mean error in the distance modulus and velocity were taken into account in calculating the depth of the supercluster. The mean thickness in Region A is 20 Mpc, which is somewhat smaller than the thickness of 26 Mpc in Region B.

There is no obvious symmetry in the Southern Supercluster either about a plane, line, or a point. If one considers only Region A, then there is a strong resemblance to a disk. However, the Southern Supercluster is not confined to Region A; it continues into Region B, becoming splayed as it approaches the supergalactic equator. If one considers the supercluster in both regions A and B there is no conventional, simple geometrical figure to describe it. The best analogy that comes to mind is a curved wedge that is narrow and thin at one end but broad and thick at the other.

VII. GROUPS

There are several groups, clouds, and clusters in the area under study. The question is: Which ones belong to the supercluster and which are foreground or background objects? The group lists published by Huchra and Geller (1982, Paper I; 1983, Paper III) were used for the identification of groups belonging to the supercluster.

From the database, only those members that had velocity information were included in this analysis. The mean position, mean velocity and its dispersion, mean angular separation and its dispersion, and mean distance modulus and its dispersion were calculated for each group as originally defined by Huchra and Geller. Since there was new velocity information, to find additional members for each of the groups the following technique was used: From the center of a particular group a circular area of the sky was searched, and simultaneously around the mean velocity of that group a range of velocity was scanned. The diameter of the areal search was the mean separation of the galaxies in the group plus 3 times its dispersion. The velocity range that was scanned was $\pm 3\sigma_v$ (where σ_v is the velocity dispersion) from the mean velocity. All the galaxies in that volume of space were listed. The new members were individually checked. If two groups had the same galaxy, a decision was made on a case-by-case basis as to which group it belonged.

After the addition of new members to the groups, the mean values of their positions, velocities, angular separations, distance moduli, and their respective dispersions were recalculated. The results are shown in Table VI. The Roman numerals I and III denote the list of Huchra and Geller in which a group is present and the Arabic numeral is the group number in that list. The mean distance modulus of a group was assigned as distance modulus to all the members of that group; in effect, the depth of the group was neglected. Group III.21 did not have any distance modulus estimate. From its average velocity and the mean Hubble ratio in that region a representative distance modulus was derived. There are at least 15 groups from the combined lists in Papers I and III of Huchra and Geller that belong to the supercluster. The richest group (or cluster) is the Fornax Cluster. The average number of galaxies per group is 15. The number of galaxies denoted in a group is a lower limit to the actual number that form a group, since the selection for group members was done only among galaxies having radial velocities.

TABLE VI. A list of groups in the Supercluster.

Group No.	<RA>	<DEC>	N_G	$<V_c>$ km/s	σ_v km/s	μ
I.01	0728.6	-6904	4	1256	66	32.07
I.03	0434.8	-5751	30	1063	231	31.29
I.06	0320.2	-5205	4	836	24	31.18
I.08	0351.2	-4526	21	831	200	30.78
I.17	0333.5	-3505	79	1161	316	31.31
I.25	0410.2	-3300	2	900	30	31.02
I.30	0313.1	-2556	7	1334	147	31.35
I.32	0328.3	-2044	37	1313	193	31.45
I.44	0237.4	-0754	10	1043	101	31.31
I.45	0131.8	-0728	5	1484	31	31.58
I.48	0240.4	+0018	5	848	182	30.53
III.12	0119.7	+0410	9	1873	88	31.85
III.13	0121.4	+0914	10	2079	193	32.66
III.21	0148.3	+0510	3	1246	125	
III.28	0224.4	-0129	6	1186	128	31.19

VIII. LUMINOSITY FUNCTION

According to its strict definition, the luminosity function gives the number of galaxies per unit interval of luminosity per unit volume. For practical purposes the luminosity function is expressed as the number of galaxies per unit of absolute-magnitude interval per unit volume. Since the volume of the supercluster has not been determined, what has been expressed is the luminosity distribution and not the luminosity function. However, the two terms will be used interchangeably since the same finite volume is being referred to in all the cases.

From the total magnitude B_T, the corrected face-on magnitude B_T^0 was derived using the formulas in RC2. The absolute magnitude was then calculated from

$$-M_T^0 = \mu - B_T^0.$$

The absolute magnitude was obtained for galaxies in three datasets—galaxies in groups, field galaxies, and all galaxies. Within the errors, there was no significant difference in the luminosity distribution in groups and field galaxies. Moreover, when the samples were further subdivided into early and late types there was no significant difference between the two. The mean absolute magnitude for the whole sample was -19.4, with a standard deviation of 1.2 mag. The histogram of the luminosity distribution for all the galaxies is shown in Fig. 6. The form of the histogram depicting the luminosity distribution suggested that a Gaussian might be a better representative expression than the Schechter function. Our results agree qualitatively with that found by Jones *et al.* (1980) in their study of the Fornax Cluster.

One of the least complete parameters in the database was the total magnitude B_T. The incompleteness factor of this parameter was obtained as a function of log D. An expression for the incompleteness factor in terms of absolute magnitude was later derived. From the actual luminosity distribution, the number of galaxies in an absolute-magnitude interval in the sample was obtained. These numbers were corrected for incomplete sampling by dividing by the incompleteness factor. Having calculated the corrected number of galaxies, the light contributed by them was obtained in solar units. The total-luminosity estimations are shown in Table VII.

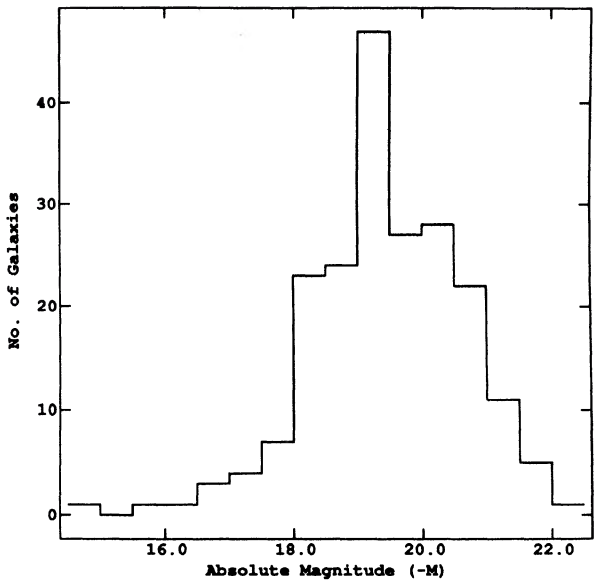

FIG. 6. Luminosity distribution of galaxies in regions A and B.

Even though the number of faint galaxies was vastly greater than the bright ones, the main contribution to the light came from the bright galaxies. The total luminosity as estimated above is a lower limit of the total luminosity of the supercluster because the incompleteness factor was derived under the assumption that the galaxies are distributed uniformly in space. There was no simple way to estimate the amount of correction necessary due to nonuniform distribution.

IX. MASS DETERMINATION

Using the virial theorem is one way of calculating the total mass in a group. Implicit in this usage is the assumption that the group is relaxed. But *a priori* that is not known. If the crossing time within the group is much smaller than the Hubble time, then it is reasonable to assume that there have been sufficient encounters to produce a relaxed system (e.g., Huchra *et al.* 1982).

Let V_G be the mean velocity of the group and n_G the number of galaxies in it. Then the velocity dispersion σ_v is given by

$$\sigma_v = \left[\sum (V_i - V_G)^2 \Big/ (n_G - 1)\right]^{1/2}.$$

If the distance of the group in Mpc is Δ obtained from the mean distance modulus, the harmonic radius of the group r_H in Mpc is expressed by

$$r_H = (\pi/2)\Delta \sin \phi,$$

where ϕ is the mean harmonic angular separation of group members

TABLE VII. Estimation of the total light.

	Before Corr N	Before Corr $L_\odot$	After Corr N	After Corr $L_\odot$
Groups	132	9.41×10^{11}	452	1.48×10^{12}
Field	72	3.94×10^{11}	1734	9.49×10^{11}
All	204	1.33×10^{12}	2186	2.43×10^{12}

$$\phi = \frac{n_G(n_G-1)}{2} \quad \frac{1}{\Sigma\Sigma\, 1/\theta_{ij}}$$

and θ_{ij} is the angular separation between any two members. The mean pairwise separation r_P in Mpc is given by

$$r_P = \frac{8}{\pi}\Delta \sin\left[\frac{\Sigma\Sigma\,\theta_{ij}}{n_G(n_G-1)}\right].$$

The crossing time T_c is expressed by

$$T_c = 3r_H/(5^{3/2}\sigma_v).$$

The virial mass of the group in solar units can be calculated from

$$\mathcal{M}_{VT} = 6.96\times 10^8 \sigma_v^2 r_H,$$

where σ_v is in km/s and r_H is in Mpc. The total apparent magnitude of the system is

$$m_t = -2.5\log\left(\sum l_i\right).$$

where $l_i = 10^{-0.4m_i}$ is the apparent luminosity of the ith galaxy. In this case m_i is the corrected face-on magnitude B_T^0 for the galaxy. The total luminosity of the group in solar units can be obtained from

$$L_T = \sum 10^{-0.4(M_i - M_\odot)},$$

where M_i is the absolute magnitude (M_T^0) of the ith galaxy and $M_\odot$ is the absolute magnitude of the Sun in the blue band. The absolute magnitude of the Sun was taken to be $M_\odot = +5.48$ (Allen 1973).

The group number, mean harmonic radius in Mpc, mean pairwise separation in Mpc, the crossing time in units of the Hubble time, the total apparent magnitude in the B band, the virial mass in solar units, the total luminosity in solar units, and the mass-to-light ratio are given in Table VIII. The mean fractional errors for the mass, luminosity, and mass-to-light ratio are 0.21, 0.30, and 0.55, respectively. The total mass for the groups was $1.5\times 10^{14}\,\mathcal{M}_\odot$ and the total luminosity was $1.5\times 10^{12}\,L_\odot$. The mean mass-to-light ratio was 100.

The mass-to-light ratio for groups provides information on the distribution of matter on a scale of $\sim$1 Mpc. But a supercluster is on a scale of tens of Mpc. Since there was no trend in the mass-to-light ratio with the size of groups under study, the mean mass-to-light of the groups was adopted as the mass-to-light ratio of the supercluster. The total corrected luminosity of the supercluster was $2.4\times 10^{12}\,L_\odot$. Hence the total mass of the supercluster was estimated to be $2.4\times 10^{14}\,\mathcal{M}_\odot$.

Several investigators (Rood *et al.* 1978; Tully 1987) have pointed out that the mass-to-light ratio increases from individual galaxies to binaries to groups to clusters. Hence the mass determined in the above analysis is a lower limit of the mass of the supercluster since we did not extrapolate. Moreover, there may be a large number of galaxies having low surface brightness and/or small angular size ($\leqslant$1′ arc) that were missed by the catalogers. (An angular size of 1′ arc corresponds to $\sim$6 kpc at the supercluster distance.)

TABLE VIII. Mass and light determination in groups.

Group	r_H	r_P	T_c	m_t	Log M_{VT}	Log L_T	M_{VT}/L_T
I.01	0.32	0.57	0.08	10.66	11.80	10.66	14
I.03	1.31	2.28	0.01	7.96	13.49	11.30	155
I.06	1.19	1.12	0.87	10.98	11.47	10.07	25
I.08	1.19	1.60	0.10	8.57	13.32	10.84	307
I.17	0.87	1.29	0.05	7.55	13.59	11.44	139
I.25	0.01	0.01	0.01	10.60	9.68	10.21	0.3?
I.30	0.78	0.90	0.09	10.09	12.87	10.48	246
I.32	1.58	2.44	0.14	8.12	13.42	11.29	136
I.44	0.47	0.64	0.08	9.64	12.34	10.63	50
I.45	0.38	0.45	0.21	10.28	11.23	10.44	6
I.48	0.38	0.37	0.04	9.15	12.75	10.51	171
III.12	0.58	1.25	0.11	10.07	12.30	10.67	43
III.13	0.37	0.39	0.03	10.71	12.79	10.75	110
III.21	0.51	0.66	0.07	11.25	12.55	10.07	304
III.28	0.28	0.42	0.04	10.40	12.31	10.31	101

TABLE IX. Description of the Southern Supercluster.

i) Location in the sky : There are two segments of the supercluster
  a) One lies between 180° ≤ L ≤ 310°, -30° ≥ B ≥ -50°, and is almost parallel to the supergalactic plane; it is the richest part of the system
  b) The other is between 270° ≤ L ≤ 320°, 0° ≥ B ≥ -30°, and is almost perpendicular to the supergalactic plane.
ii) Location in velocity space : The range of velocities is
  2.75 ≤ log V_c ≤ 3.35
  560 ≤ V_c km/s ≤ 2240
iii) Mean Distance (to the center of light) : 19.5 Mpc
iv) Longest angular dimension (along the length of the supercluster) : 123°
v) Longest linear dimension (along the length of the supercluster) : 41 Mpc
vi) Shape : The supercluster is neither a disk nor a filament. It lies on a curved two-dimensional surface and varies non-uniformly in thickness.
vii) Number of galaxies : The number of galaxies (after correcting for incompleteness) that are bigger than 1′ of arc in diameter or brighter than 15th mag is ~1500.
viii) Number of groups : 15
ix) Percentage of galaxies in groups : 64%
x) Total Luminosity : $2.4\times 10^{12}\,h^{-2}L_\odot$
xi) Mean mass-to-light ratio : 100 h ($M_\odot/L_\odot$)
xii) Total mass : $2.4\times 10^{14}\,h^{-1}M_\odot$

X. SUMMARY AND CONCLUSIONS

A concise description of the Southern Supercluster has been given in Table IX. How does the Southern Supercluster compare with other superclusters? To allow for the various distance scales of different authors, all results have been expressed in terms of h, where $h = H_0/100$. However, the limiting magnitudes and the methods of mass determination were different for the various investigators. The total mass, luminosity, and the mean mass-to-light ratio for the Perseus, Coma, Hercules, and the Southern superclusters have been given in Table X for comparison. Only the total mass for the Local Supercluster was readily available. The Perseus Su-

TABLE X. Comparison with other superclusters.

Supercluster	$(h^{-1})M_\odot$	$(h^{-2})L_\odot$	$(h)M_\odot/L_\odot$	Reference
Local	1.5×10^{15}			de Vaucouleurs (1958)
Perseus	1.4×10^{16}	4.5×10^{13}	308	Einasto et al. (1980)
Coma	6.3×10^{14}	2.0×10^{12}	329	Gregory et al. (1978)
Hercules	2.0×10^{14}	9.0×10^{12}	22	Tarenghi et al. (1980)
Southern	2.4×10^{14}	2.4×10^{12}	100	

percluster is a giant among superclusters. The Southern Supercluster compares well (in terms of mass, luminosity, and mass-to-light ratio) with the Coma and Hercules superclusters but is less massive than the Local Supercluster.

Since the Southern Supercluster is the nearest supercluster to the Local Supercluster, there were reasons to believe that there was some connection between the two. When one looks at an all-sky map in supergalactic coordinates one sees a segment of the Southern Supercluster stretching to the supergalactic equator. However, the Southern Supercluster is well defined on the low-velocity side in velocity space. The segment that reaches to the supergalactic plane gets further out in space the closer one approaches the equator. So the Southern Supercluster is well separated from the Local Supercluster.

When one superimposes the polar diagrams in slices parallel and perpendicular to the supergalactic equator in Region B there is evidence of a tenuous stream of galaxies connecting the Southern Supercluster with the Perseus Supercluster. The reality of this stream of galaxies cannot be doubted. However, whether such a low-density filament can be called a connecting link is a semantic question.

Does the Southern Supercluster end at the angular limits imposed? In Region A one end of the supercluster runs into the Milky Way. It would be difficult to determine how far across the plane of the Milky Way it extends. One possibility would be to make infrared or 21 cm H I observations along an extension of the densest plane of the supercluster. The other possibility would be to look for galaxies on the other side of the Milky Way but in the same velocity range as the supercluster.

In Region B one segment of the supercluster meets the supergalactic equator, which was one of the limits imposed by this study. Using the new CfA redshift catalog, all-sky maps were generated in the velocity range of the supercluster. These maps show that the supercluster does indeed extend to positive supergalactic latitude. However, the density of galaxies diminishes rapidly. The addition of this extension would naturally cause revisions in the estimates of length, luminosity, mass, etc.

I would like to thank Professor G. de Vaucouleurs for his guidance and encouragement throughout this project and Dr. Harold Corwin for his helpful comments and careful reading of this paper. My thanks are also to Dr. John Huchra for sending me a subset of the CfA redshift catalog for my analysis.

REFERENCES

Allen, C. W. (1973). *Astrophysical Quantities*, 3rd edition (Athlone, London).

Bottinelli, L., Gouguenheim, L., Paturel, G., and de Vaucouleurs, G. (1983). Astron Astrophys. **118**, 4.

Corwin, H. G., Jr., de Vaucouleurs, A., and de Vaucouleurs, G. (1985). *Southern Galaxy Catalogue*, Monogr. Astron. No. 4 (The University of Texas, Austin).

de Vaucouleurs, G. (1953). Astron. J. **58**, 30.

de Vaucouleurs, G. (1956). Vistas Astron. **2**, 1584.

de Vaucouleurs, G. (1958). Astron. J. **63**, 253.

de Vaucouleurs, G. (1979). Astrophys. J. **227**, 380.

de Vaucouleurs, G., and Buta, R. (1980a). Astrophys. J. Suppl. **44**, 451.

de Vaucouleurs, G., and Buta, R. (1980b). Astron. J. **85**, 637.

de Vaucouleurs, G., and Olson, D. W. (1982). Astrophys. J. **256**, 346.

de Vaucouleurs, G., de Vaucouleurs, A., and Corwin, H. G., Jr. (1976). *Second Reference Catalogue of Bright Galaxies* (University of Texas, Austin).

Einasto, J., Joeveer, M., and Saar, E. (1980). Mon. Not. R. Astron. Soc. **193**, 353.

Faber, S. M., and Jackson, R. E. (1976). Astrophys. J. **204**, 668.

Geller, M. J., and Huchra, J. P. (1983). Astrophys. J. Suppl. **52**, 61 (Paper III).

Gregory, S. A., and Thompson, L. A. (1978). Astrophys. J. **222**, 784.

Herschel, J. W. (1847). *Results...Cape of Good Hope* (Smith, Elder, and Co., London).

Huchra, J. P., and Geller, M. J. (1982). Astrophys. J. **257**, 423 (Paper I).

Jones, J. E., and Jones, B. J. T. (1980). Mon. Not. R. Astron. Soc. **191**, 685.

Lauberts, A. (1982). *The ESO/Uppsala Survey of the ESO(B) Atlas* (European Southern Observatory, Munich).

Nilson, P. (1973a). *Uppsala General Catalogue of Galaxies* (Almqvist and Wiksell, Stockholm).

Nilson, P. (1973b). *Catalogue of Selected non-UGC Galaxies* (Almqvist and Wiksell, Stockholm).

Palumbo, G. G. C., Tanzella-Nitti, G., and Vettolani, G. (1983). *Catalogue of Radial Velocities of Galaxies* (Gordon and Breach, New York).

Paturel, G. (1981). Doctoral thesis, University of Lyon.

Richter, O. G., and Sadler, E. M. (1985). Astron. Astrophys. Suppl. **59**, 433.

Rood, H. J. (1975). Astrophys. J. **201**, 551.

Rood, H. J., and Dickel, J. R. (1978). Astrophys. J. **224**, 724.

Tarenghi, M., Chincarini, G., Rood, H. J., and Thompson, L. A. (1980). Astrophys. J. **235**, 724.

Tully, R. B. (1987). Astrophys. J. **321**, 280.

Tully, R. B., and Fisher, J. R. (1977). Astron. Astrophys. **54**, 661.

Welch, G. A., Chincarini, G., and Rood, H. J. (1975). Astron. J. **80**, 77.